

# A comparative study between the monitored and simulated response of a monopile located in the Belgian North Sea

A. Kheffache

*Ghent University, Ghent, Zwijnaarde 9052, Belgium.*

B. Stuyts

*Ghent University, Ghent, Zwijnaarde 9052, Belgium.*

**ABSTRACT:** This paper presents the results of a comparative study between the monitored and the simulated response of a monitored wind turbine monopile located in the Belgian North Sea, subjected to operational lateral loading. A 3D Finite Element model of the monopile is developed in ABAQUS in which the soil is simulated using advanced constitutive models for sands and clays that are calibrated to advanced laboratory test data. It is found that using a stiffness profile that is calibrated from laboratory tests only induces the most mismatch when compared to the monitoring data. The effect of CPT-based  $G_{max}$  correlations was also investigated, it was concluded that it was not the main reason behind the observed mismatch between the numerical models and the monitoring data.

## 1 INTRODUCTION

As most European countries are aiming to an increase of the total installed offshore wind capacity, monopile-supported wind turbines are getting more attention, with an emphasis on lifetime extension of the currently installed ones, but also design optimization for next generation wind turbines foundations. Monopile-supported offshore wind turbines represent more than 80% of the total installed foundations.

The design recommendations from the Oil and Gas (O&G) industry (API, 2011; DNV, 2014) were used to design the first generation of wind turbine monopiles. The soil is modelled using non linear springs; the so called  $p$ - $y$  curves. Such approaches are particularly attractive, as they are not computationally demanding, which makes them well adopted in the industry. The recommendations have been proven to not be adapted for the design of high diameter piles (such as monopiles), as they were initially formulated for more slender piles, typically used for offshore O&G structures (Doherty & Gavin, 2012). The PISA design methodology for laterally piles in sands and clays (Burd et al., 2020; Byrne et al., 2020), is a new approach that is currently used for the design of large diameter monopiles. It introduced new sets of reaction curves such as the moment-rotation, base moment and base shear curves. 3D Finite Element (FE) modelling approaches are computationally more costly than the 1D ones, however they are better at modelling the complex soil-monopile interactions, given that the soil constitutive model is properly calibrated and adapted for the problem at hand.

Offshore wind turbines are dynamic-sensitive structures, their natural frequency  $f_0$  is generally designed to fall in the soft-stiff range where it is surrounded by forcing frequencies, such as the higher blade (3P) and lower rotor (1P), wave and wind frequencies (Figure 1). Any shift of  $f_0$  towards one of the excitation frequencies could induce damage in the structural steel due to resonance. The stiffness of offshore wind turbines is from this point of view capital. While the wind turbine structure is a major contributor to its stiffness through its bending stiffness (contribution of diameter, thickness and Young's modulus), the soil is a non-negligible contributor to the overall lateral stiffness. The soil surrounding the monopile is also a major source of uncertainty, which makes the exact design of wind turbines according to the soft-stiff range a difficult task. Future

wind turbines are going to be installed in deeper waters, bringing their natural frequency even closer to the wave frequency range. Moreover, Figure 2 shows the evolution of the target frequency range for several wind turbines from many wind farms in the UK and the Netherlands, a clear shift towards the lower wave frequency is noticed, as the turbines keep increasing in size (due to the increase in rotor diameter), which makes the exact determination of wind turbines stiffness even more critical.

In this work, 3D FE modelling of a monitored wind turbine monopile is carried. A site-specific ABAQUS model is developed, in which the hypoplastic constitutive models are assigned to the soil. Two modelling approaches are followed, first, the models are calibrated using advanced laboratory test only. The calibration is then optimized using in-situ test data carried near the monitored wind turbine location, taking into account the uncertainty. The effect of each approach on the modelling outcomes are investigated using the monitoring data. Conclusions are drawn and recommendations are formulated.

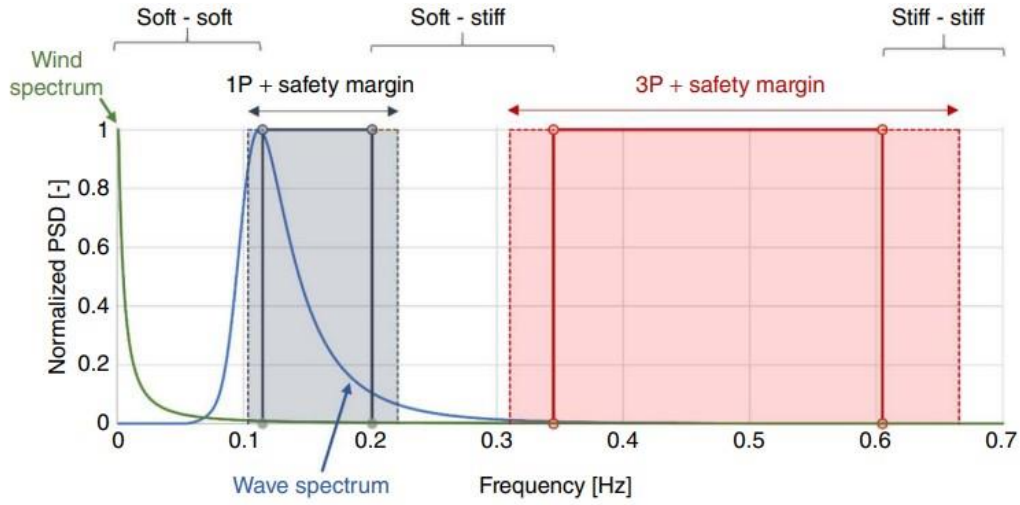


Figure 1. Spectrum of wind, wave, 1P and 3P frequencies (Bhattacharya, 2019)

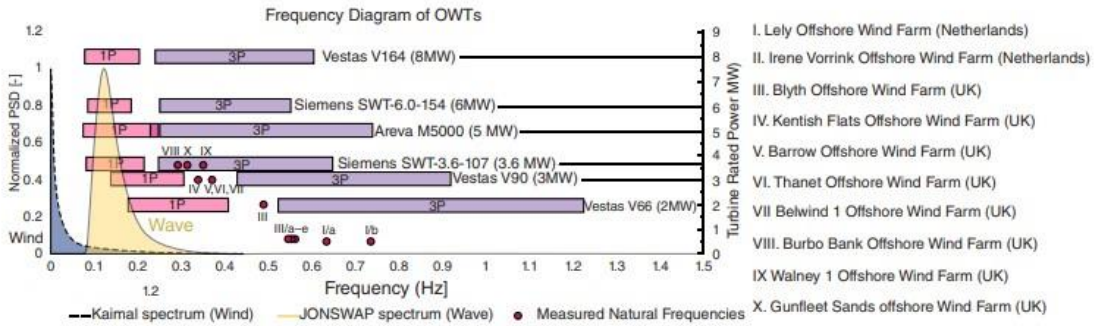


Figure 2. Evolution of wind turbines frequencies across multiple wind farms (Bhattacharya, 2019)

## 2 SITE CONDITIONS

### 2.1 Monopile

The studied monopile is located in the Belgian North Sea. The monopile diameter  $D$ , stick-up length  $h$ , penetration depth  $L$ , wall thickness  $t$ , water depth are given in Table 1. The monopile

was also equipped with Fiber Bragg Gratings (FBGs) that measure the strains on the monopile part. The FBGs were positioned at depths of 1, 3 and 6m below the mudline level (Figure 3).

*Table 1. Monopile geometry*

h (m)	L (m)	t (mm)	Water depth (m)	D (m)
37	29.9	57-95	32	5

## 2.2 Soil conditions

The monopile is embedded in a two-layered soil medium where the first 8m is a medium-dense quaternary sand, the lower soil part is made of overconsolidated tertiary clay, that may include a descent amount of sandy layers. This layering is typical in the Belgian North Sea, the top layer sand tends to increase in thickness in the north-east, while the clay layer rises to the mudline level towards the south-west direction. The piezocone penetration test (CPTu), soil profile at the wind turbine's location are shown in Figure 3.

## 2.3 Loads

Representative sets of loadings were extracted from the monitoring data (10-minutes strain measurements) available on the upper structure (above mudline part of the wind turbine). The derived loading consists of a point force and moment applied at the head of the monopile. A total of 26 load conditions are considered in this work. The loads are considered to be quasi-static; the loads were extracted from episodes where the wind turbine was operating under normal conditions and where the strain measurements were seen to have relatively small variations. The thickness of the top sand is within the reported thicknesses reported in the wind turbine region by (Le Bot et al., 2003)

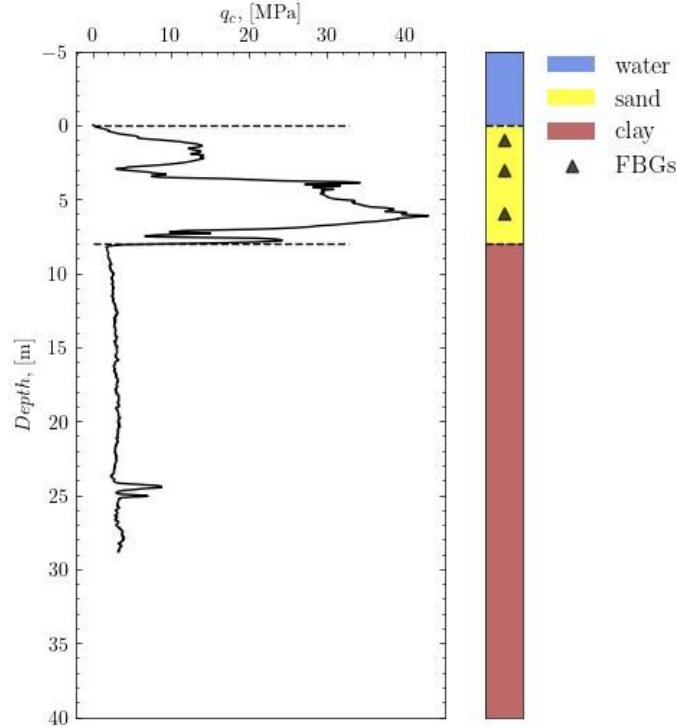


*Figure 3. CPT, FBGs and soil layering at the wind turbine's location.*

### 3 FE MODELLING

#### 3.1 Soil

The soil sand and clay layers are modelled using the hypoplastic models (Mařín, 2013; von Wolffersdorff, 1996). The constitutive models have been previously calibrated (Kheffache et al., 2023), the calibration is not repeated here for brevity. The constitutive models are first calibrated using the available laboratory test data, performed on soil samples that were extracted from boreholes close to the wind turbine location. The calibration is then optimized using in-situ test data that consists of Seismic CPT (SPCTu) and CPT measurements around the wind turbine location. The measured and calibrated  $G_{max}$  profiles are shown in Figure 4, the values below 30m (depth at which the CPT data stops) were extrapolated from nearby borehole-CPT which can go up to 60m depth. The CPT-based  $G_{max}$  profile was calculated using the Robertson & Cabal (2015) correlation, for which a 90% confidence interval was established according to the following equation assuming that  $G_{max,M}/G_{max,R}$  is normally distributed:

$$G_{max,R} = \frac{G_{max,M}}{\mu.(1 \pm 1.645.COV)} \quad (1)$$

where  $G_{max,R}$  and  $G_{max,M}$  are the real and the measured stiffness values (interpreted from SCPT shear wave velocity data),  $\mu$  is the mean of statistical distribution and  $COV$  is the coefficient of variation. The  $G_{max}$  measured in laboratory using bender element (BE) and resonant column (RC) tests usually fall on the lower end of the values measured in-situ (Gomez Bautista & Stuyts, 2022). The effect of each  $G_{max}$  profile (laboratory, best estimate and 90% CI) on the numerical bending moments will be investigated in what follows.

The soil stress was initialized using a  $K_0$  initial stress state, where  $K_0$  is the coefficient of earth pressure at rest, calculated using the following equation:

$$K_0 = (1 - \sin \varphi_c)OCR^{\sin \varphi_c} \quad (2)$$

Where  $\varphi_c$  is the critical state friction angle and  $OCR$  is the overconsolidation ratio, interpreted using oedometer tests. The sand initial void ratio was established using water content measurements.

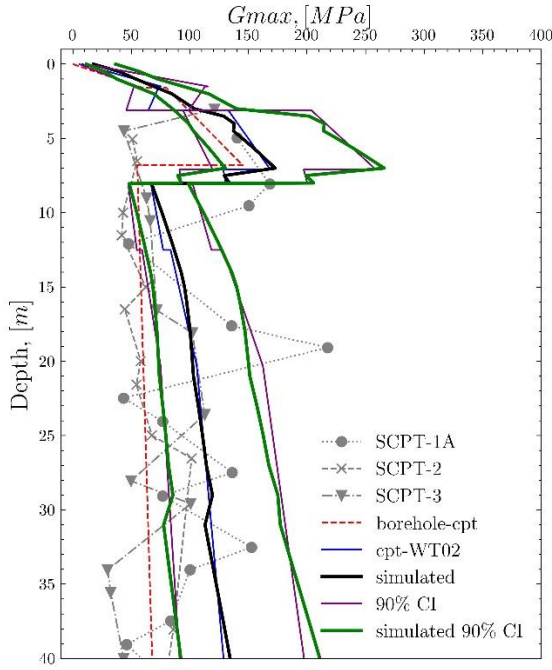


Figure 4. Calibrated  $G_{max}$  profiles

### 3.2 Monopile

The monopile is modelled using C3D8I mesh elements which are incompatible 3D continuum 8 noded fully integrated linear brick elements, recommended for solid elements subject to bending (Abaqus, 2011). A comparative study was done by comparing C3D8I elements to S4R (shell) bending moments, negligible differences were observed.

### 3.3 Boundary conditions

Only half of the model is modelled, taking advantage of symmetry. The symmetry plane is fixed in the normal direction (horizontal). The outer model is fixed in all directions except the vertical. The model is fixed in all directions at the bottom.

### 3.4 Interface

The tangential interface behaviour is modelled using a Mohr-Coulomb friction coefficient  $\mu$ . The calculated values for the sand and clay layers were between 0.3 and 0.5, a sensitivity analysis was performed on  $\mu$  values which indicated that this parameter had no effect on the computed bending moments. A uniform value of  $\mu=0.5$  was adopted along the monopile. The normal contact behaviour was modelled using the 'hard' contact pressure overclosure relationship.

## 4 RESULTS AND DISCUSSION

The monitored and simulated bending moments are given in normalized form in Figure 5, only 3 out of the total moments are shown for clarity. For all the considered cases, all the computed bending moments are positioned at the right of the monitored ones, expressing an overestimation. The moment profiles corresponding to the best estimate of  $G_{max}$  are surrounded by the 90% confidence interval ones. The moments computed using laboratory  $G_{max}$  values are the highest. The effect of soil stiffness (through the  $G_{max}$  profile) can directly be seen on the bending moments, as the increase of  $G_{max}$  induced a decrease in the computed bending moments.

The mean relative error ( $MRE$ ); which is the relative error between the monitored and simulated bending moments; is expressed using the following equation:

$$MRE = \frac{1}{n} \sum_{i=0}^{n-1} \frac{M_m^{z,i} - M_s^{z,i}}{M_m^{z,i}} \quad (3)$$

where  $n$  is the total number of considered load cases (26),  $M_m^{z,i}$  is the monitored bending moment at the  $z$ -th sensor depth for the  $i$ -th load case and  $M_s^{z,i}$  is the simulated moment at the same depth and for the same load case. Negative and positive  $MRE$  values correspond to an over and under-estimation respectively. It can be seen from Figure 6 that for all the modelling cases, the minimum and maximum  $MRE$  values at each sensor depth correspond to the 90% CI and lab-only  $G_{max}$  profiles respectively. It can be seen that the  $MRE$  at the first sensor level is not influenced by any of the adopted  $G_{max}$  profiles, since the bending moment near the mudline is mainly affected by the load intensity. The effect of  $G_{max}$  is more visible on the deep sensors, especially at  $z/D$  of 6.

The general  $MRE$  ( $GMRE$ ); which is defined as the mean of the  $MRE$  values; is shown for each case in Figure 7. The  $GMRE$  allows for a direct comparison between the simulated cases. Here again, the highest and lowest  $GMRE$  values correspond to the lab-only and stiffer 90% CI  $G_{max}$  profiles respectively.

Having established the effect of soil stiffness ( $G_{max}$ ) on the monopile bending moments, the mismatch between the simulated and the monitored bending moments is certainly due to a mismatch between the in-situ and modelled soil stiffness, meaning that the in-situ monopiles are laterally stiffer than expected. This stiffness mismatch can be due to many reasons, one of them being the CPT  $G_{max}$  correlations uncertainty. The uncertainty can be ruled out since the 90% confidence interval on  $G_{max}$  was not seen to drastically affect the bending moments,  $MRE$  and  $GMRE$  values, adopting a best estimate  $G_{max}$  profile would lead to comparable results. Interestingly, the simulations based on a  $G_{max}$  profile estimated from laboratory tests only (using BE and RC tests) gave the worst results in terms of mismatch, highlighting the importance of a proper soil investigation campaign.

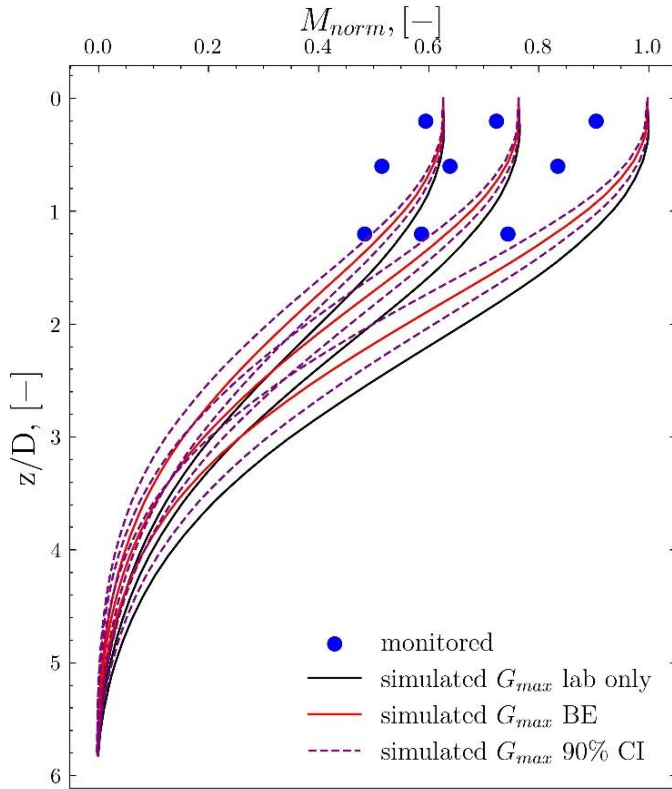


Figure 5. Simulated and monitored bending moment profiles

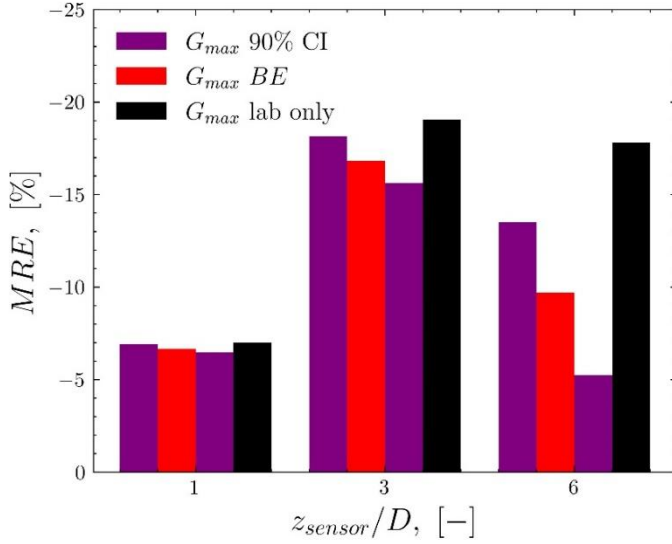


Figure 6. MRE for the simulated cases at each sensor depth

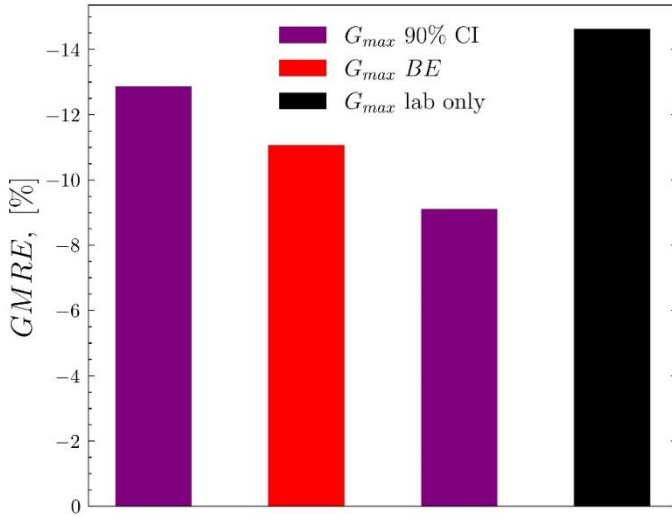


Figure 7. GMRE for the simulated cases

## 5 CONCLUSIONS AND RECOMMENDATIONS

In this work, the bending moments have been computed for a monitored wind turbine monopile that is located in the Belgian North Sea. Different soil stiffness profiles have been considered in order to investigate the effect of  $G_{\text{max}}$ . The following conclusions are drawn:

- A clear mismatch is shown between the monitored and computed bending moments, the wind turbine monopile is laterally stiffer than expected.
- The 90% confidence interval (CI) on the CPT-based  $G_{\text{max}}$  profile is not the main reason for this mismatch.
- Using laboratory tests only for the characterization of soil stiffness would lead to unrealistic values, that would impact the structural dynamics of wind turbines. A thorough soil investigation campaign is needed.

Future works are going to focus on the reason for the observed mismatch. The in-situ wind turbines are surrounded by a scour protection, which was not taken into account in the simulations. The effect of scour protection will be further investigated.

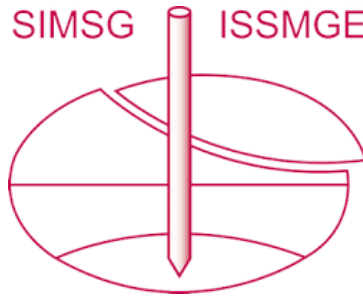
## ACKNOWLEDGEMENTS

The authors would like to acknowledge the support of the Belgian Ministry of Economic Affairs through the EFT project WINDSOIL project. The Support of VLAIO through the De Blauwe Cluster SBO SOILTWIN project is also acknowledged.

## REFERENCES

- Abaqus, G. (2011). Abaqus 6.11. *Dassault Systemes Simulia Corporation, Providence, RI, USA*, 3.
- API. (2011). *API RP2 GEO Geotechnical and Foundation Design Considerations*.
- Bhattacharya, S. (2019). *Design of Foundations for Offshore Wind Turbines* (1st ed.). Wiley. <https://doi.org/10.1002/9781119128137>
- Burd, H. J., Taborda, D. M. G., Zdravković, L., Abadie, C. N., Byrne, B. W., Houlsby, G. T., Gavin, K. G., Igoe, D. J. P., Jardine, R. J., Martin, C. M., McAdam, R. A., Pedro, A. M. G., & Potts, D. M. (2020). PISA design model for monopiles for offshore wind turbines: Application to a marine sand. *Géotechnique*, 70(11), 1048–1066. <https://doi.org/10.1680/jgeot.18.P.277>
- Byrne, B. W., Houlsby, G. T., Burd, H. J., Gavin, K. G., Igoe, D. J. P., Jardine, R. J., Martin, C. M., McAdam, R. A., Potts, D. M., Taborda, D. M. G., & Zdravković, L. (2020). PISA design model for monopiles for offshore wind turbines: Application to a stiff glacial clay till. *Géotechnique*, 70(11), 1030–1047. <https://doi.org/10.1680/jgeot.18.P.255>
- DNV. (2014). *DNV-OS-J101 Design of Offshore Wind Turbine Structures*.
- Doherty, P., & Gavin, K. (2012). Laterally loaded monopile design for offshore wind farms. *Proceedings of the Institution of Civil Engineers - Energy*, 165(1), 7–17. <https://doi.org/10.1680/ener.11.00003>
- Gomez Bautista, D. A., & Stuyts, B. (2022). Bender element testing to determine small-strain shear modulus on Belgian North Sea soils. *Proceedings of the 7th International Young Geotechnical Engineers Conference*. 7th International Young Geotechnical Engineers Conference, Sydney, Australia.
- Kheffache, A., Stuyts, B., Sastre Jurado, C., Weijtjens, W., & Devriendt, C. (2023). 3D FE simulation of an instrumented monopile under quasi-static loading. *10th European Conference on Numerical Methods in Geotechnical Engineering*. NUMGE2023, London, U.K.
- Le Bot, S., Van Lancker, V., Deleu, S., De Batist, M., & Henriët, J. (2003). *Tertiary and quaternary geology of the Belgian Continental Shelf*.
- Mašin, D. (2013). Clay hypoplasticity with explicitly defined asymptotic states. *Acta Geotechnica*, 8(5), 481–496. <https://doi.org/10.1007/s11440-012-0199-y>
- Robertson, P., & Cabal, K. L. (2015). *Guide to Cone Penetration Testing*. R:\Zotero\CA Technical references\2015 Robertson and Cabal - Guide to Cone Penetration Testing.pdf
- von Wolffersdorff, P.-A. (1996). A hypoplastic relation for granular materials with a predefined limit state surface. *Mechanics of Cohesive-Frictional Materials*, 1(3), 251–271. [https://doi.org/10.1002/\(SICI\)1099-1484\(199607\)1:3<251::AID-CFM13>3.0.CO;2-3](https://doi.org/10.1002/(SICI)1099-1484(199607)1:3<251::AID-CFM13>3.0.CO;2-3)

# INTERNATIONAL SOCIETY FOR SOIL MECHANICS AND GEOTECHNICAL ENGINEERING



*This paper was downloaded from the Online Library of the International Society for Soil Mechanics and Geotechnical Engineering (ISSMGE). The library is available here:*

<https://www.issmge.org/publications/online-library>

*This is an open-access database that archives thousands of papers published under the Auspices of the ISSMGE and maintained by the Innovation and Development Committee of ISSMGE.*

*The paper was published in the proceedings of the 18th African Regional Conference on Soil Mechanics and Geotechnical Engineering and was edited by Abdelmalek Bekkouche. The conference was held from October 6<sup>th</sup> to October 9<sup>th</sup> 2024 in Algiers, Algeria.*